Spin Caloritronics in Noncondensed Bose Gases

C. H. Wong, H. J. van Driel, R. Kittinaradorn, H. T. C. Stoof, and R. A. Duine
Institute for Theoretical Physics, Utrecht University, Leuvenlaan 4, 3584 CE Utrecht, The Netherlands
(Received 18 October 2011; published 13 February 2012)

We consider coupled spin and heat transport in a two-component atomic Bose gas in the noncondensed state. We find that the transport coefficients show a temperature dependence reflecting the bosonic enhancement of scattering and discuss experimental signatures of the spin-heat coupling in spin accumulation, spin separation, and total dissipation. Close to the critical temperature for Bose-Einstein condensation, we find that the spin-heat coupling is strongly reduced, which is also reflected in the spin caloritronics figure of merit that determines the thermodynamic efficiency of spin-heat conversion.

DOI: 10.1103/PhysRevLett.108.075301 PACS numbers: 67.85.−d, 03.75.−b, 67.10.Fj, 67.10.Jn

The Seebeck and Peltier effects are thermoelectric phenomena that are well understood for ordinary conductors. Besides being theoretically interesting, these effects have many commercial applications ranging from wine coolers to thermoelectric generators. Recent developments in spintronics have led to the nascent field of spin caloritronics [1] that introduces a spin-dependent generalization of these phenomena. In solid-state systems, the spin-Seebeck and spin-dependent Seebeck effects have recently been measured [2,3], while their theoretical explanations are still under active debate [4].

Cold-atom systems provide a perfectly clean environment to study spin caloritronics, without many of the factors that can make the interpretation of solid-state experiments difficult. In addition, cold atoms are advantageous in the study of spin and spin-resolved heat transport because one can experimentally realize systems where spin is conserved, apply different temperatures for different atomic species, and measure their distribution functions separately. While equilibrium properties of these systems have been thoroughly studied, recent research has started to focus on nonequilibrium behavior such as spin dynamics [5], heat transport [6], and spin drag [7,8]. The spin drag relaxation rate has been measured in Fermi gases [8], and experiments to measure the spin drag conductivity in Bose gases have recently been performed [9]. However, the concomitant thermospin phenomena remain largely unexplored.

In this Letter, we study the coupling of spin and heat transport in a cold atomic Bose mixture of two spin species and calculate the spin and heat transport coefficients in the noncondensed state. In particular, we show that the bosonic nature of the particles leads to qualitatively different temperature dependence of these coefficients as compared to electronic systems. Furthermore, we introduce a spin caloritronic figure of merit for this system called "Z_sT," analogous to the "ZT" figure of merit that determines the efficiency of devices based on the usual solid-state thermoelectric effect. We compute the temperature dependence of Z_sT and find a downturn on approach to the critical temperature of Bose-Einstein condensation. Our theoretical results also have implications for thermospin phenomena in other systems where the transport is mediated by degenerate bosons, such as a quasiequilibrium magnon gas [10].

We begin by considering a cold boson system above the critical temperature T_c of Bose-Einstein condensation, composed of two different spin states selected from a larger integer-spin multiplet, which we will label "spin-up" (↑) and "spin-down" (↓). We apply forces and temperature gradients which are equal and opposite for the two spin species, i.e., $\mathbf{F}_\uparrow = -\mathbf{F}_\downarrow$ and $\nabla T_\uparrow = -\nabla T_\downarrow$ [11]. In response to the "spin force" and "spin temperature gradients" defined by $\mathbf{F}_s \equiv \mathbf{F}_\uparrow - \mathbf{F}_\downarrow$ and $\nabla T_s \equiv \nabla T_\uparrow - \nabla T_\downarrow$, there will be a spin current and spin-heat current, $\mathbf{j}_s = \mathbf{j}_\uparrow - \mathbf{j}_\downarrow$ and $\mathbf{q}_s = \mathbf{q}_\uparrow - \mathbf{q}_\downarrow$, respectively. We define the linear-response coefficients by (shown schematically in Fig. 1) :

$$\begin{pmatrix} \mathbf{j}_s \\ \mathbf{q}_s \end{pmatrix} = \begin{pmatrix} \sigma_s & \sigma_s S_s \\ \sigma_s P_s & \kappa_s' \end{pmatrix} \begin{pmatrix} \mathbf{F}_s \\ -\nabla T_s \end{pmatrix}. \tag{1}$$

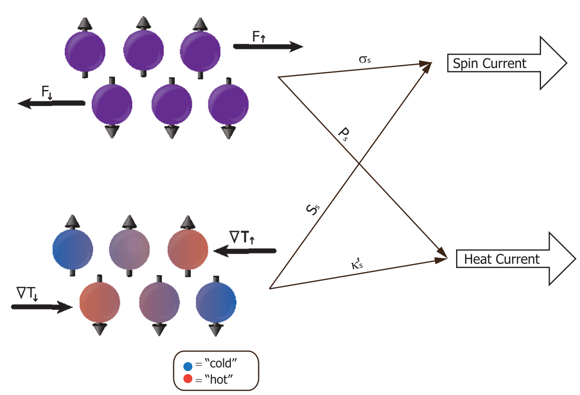

FIG. 1 (color online). Schematic illustration of the coupled spin and heat transport. Spin-dependent forces or temperature gradients, labeled by $\mathbf{F}_{\uparrow,\downarrow}$, $\nabla T_{\uparrow,\downarrow}$, generate both spin and spin-heat currents proportional to the coefficients σ_s and P_s in the former and κ_s and S_s in the latter case, as illustrated in the figure.

 © 2012 American Physical Society

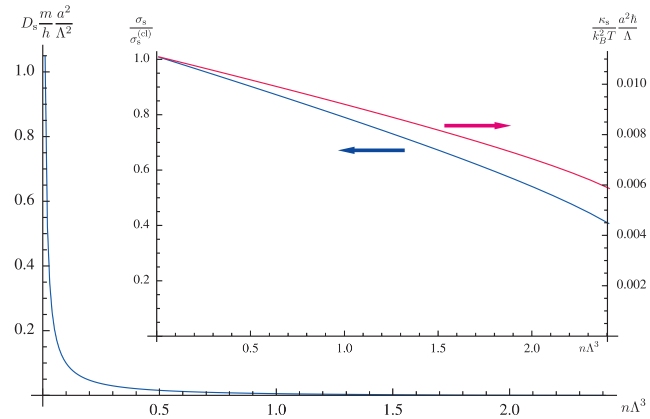

FIG. 2 (color online). Spin diffusivity [normalized by $(h/m)\times(\Lambda^2/a^2)$] as a function of the degeneracy parameter $n\Lambda^3$. Inset: A plot of the spin conductivity σ_s relative to the classical value (left axes) $\sigma_s^{(cl)} = (3/64\sqrt{2}\pi)(\Lambda/a^2\hbar)$ and a plot of the spin-heat conductivity at zero spin current, κ_s, normalized by $k_B^2 T\Lambda/a^2\hbar$ (right axis).

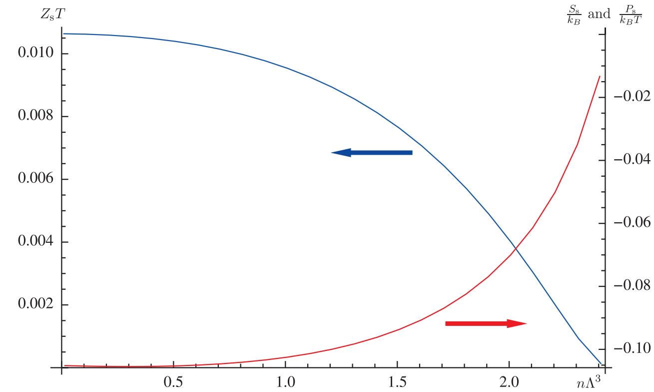

FIG. 3 (color online). Spin-Seebeck coefficient in units of k_B (right axis) and the dimensionless figure of merit $Z_s T$ (left axis). The plots here are outside the critical region, where the absolute magnitude of both coefficients decreases with temperature on the approach to the critical point (note that the values of S_s are negative).

In the above, σ_s is the spin conductivity, κ_s' is the spin-heat conductivity at zero $\mathbf{F}_s$, and S_s and P_s are the spin-Seebeck and spin-Peltier coefficients, respectively, which are related by the Onsager reciprocity principle, $P_s = S_s T$, T being the temperature. Although we have written the response matrix in a form analogous to the thermoelectric coefficients defined in metals, here the microscopic mechanisms for the coupling between spin and heat flows are different from those in metals because there are no disorder and lattice phonons in the Bose gas. The spin-heat coupling studied here is akin to the thermodiffusion effect in multicomponent classical gases [12]. The spin conductivity is, to the leading order, determined by the viscosity between up and down atoms that arises from interspin scattering, which is called spin drag. In contrast, the spin-heat conductivity, which has dependence on intraspin scattering, is finite even in the absence of interspin scattering.

Using the Boltzmann equation for a two-component Bose gas, we have computed σ_s, κ_s', and S_s as a function of $n\Lambda^3$, with n the equilibrium particle density per spin state that is assumed to be equal for both spin species and $\Lambda = \sqrt{2\pi\hbar^2/mk_BT}$ the thermal de Broglie wavelength, where m is the particle mass, $\hbar$ is the Planck's constant, and k_B the Boltzmann constant. The results are shown in Figs. 2 (inset) and 3. The order of magnitude of the Seebeck coefficient is $S_s \sim -0.01k_B \sim -1\ \mu\text{eV/K}$, comparable to what is found in ferromagnetic materials [3]. Notable is the sharp decrease of all transport coefficients as one approaches the critical value $n\Lambda^3 \simeq 2.61$. This effect is due to bosonic enhancement of scattering into occupied states, which dramatically increases as one approaches the critical temperature $T_c = 2\pi\hbar^2/mk_B\Lambda_c^2$, where $\Lambda_c \simeq (2.61/n)^{1/3}$. This effect is illustrated in Fig. 4, where we plot the effective relative momentum distribution f_{rel}, defined so that the interspin collision rate is given by $1/\tau_{\text{inter}} = \sigma_{\text{inter}} \int p_r^2 dp_r v_r f_{\text{rel}}(p_r)/(2\pi\hbar)^3$, where $\sigma_{\text{inter}} = 4\pi a^2$ is the interspin scattering cross section and v_r the relative velocity. As shown in the figure, this distribution increases sharply as one approaches the critical temperature. This is in contrast to spin drag in degenerate Fermi gases, where due to Pauli blocking, below the Fermi temperature the spin conductivity increases as the temperature is lowered [13].

Next we outline the calculation of the transport coefficients. We start with the two-component, static Boltzmann equation for the semiclassical distribution function $n_{\mathbf{p}\sigma}(\mathbf{r})$ under spin-dependent external forces $\mathbf{f}_\sigma$,

$$(\mathbf{v_p}\cdot\nabla + \mathbf{f}_\sigma\cdot\nabla_\mathbf{p})n_{\mathbf{p}\sigma} = C_{\mathbf{p}\sigma}[n_\uparrow, n_\downarrow], \tag{2}$$

where $\mathbf{v_p} = \mathbf{p}/m$ is the particle velocity, $\sigma = \uparrow, \downarrow$ the (pseudo)spin of the two-component Bose gas, and the collision integrals C_σ are given by

$$C_{\mathbf{p}_1\sigma}[n_\uparrow, n_\downarrow] = -\int \frac{d\mathbf{p}_2}{(2\pi\hbar)^3}|\mathbf{v}_{\mathbf{p}_1} - \mathbf{v}_{\mathbf{p}_2}| \int d\Omega_r' \sum_{\tau=\uparrow,\downarrow} \frac{d\sigma_{\sigma\tau}}{d\Omega_r'} \times [n_{1\sigma}n_{2\tau}(1+n_{3\sigma})(1+n_{4\tau}) - n_{3\sigma}n_{4\tau}(1+n_{1\sigma})(1+n_{2\tau})]. \tag{3}$$

The collision integral describes the 2-body elastic scattering of particles labeled by $(\mathbf{p}_1\sigma, \mathbf{p}_2\tau) \to (\mathbf{p}_3\sigma, \mathbf{p}_4\tau)$, and Ω' is the solid angle between ingoing and outgoing relative momenta $\mathbf{p}_r = (\mathbf{p}_1 - \mathbf{p}_2)/2$ and $\mathbf{p}_r' = (\mathbf{p}_3 - \mathbf{p}_4)/2$, respectively. We take the interspin differential cross section to be $d\sigma_{\uparrow\downarrow}/d\Omega_{\text{inter}} = a^2$, where a is the scattering length, and take the intraspin terms to be $d\sigma_{\uparrow\uparrow}/d\Omega = d\sigma_{\downarrow\downarrow}/d\Omega = 2a^2$ on account of Bose statistics [14]. We parametrize the nonequilibrium, steady state distribution by

$$n_{\mathbf{p}\sigma}(\mathbf{r}) = f_{\mathbf{p}\sigma}(\mathbf{r}) - \partial_\epsilon f_\mathbf{p}^0 \phi_{\mathbf{p}\sigma}(\mathbf{r}), \tag{4}$$

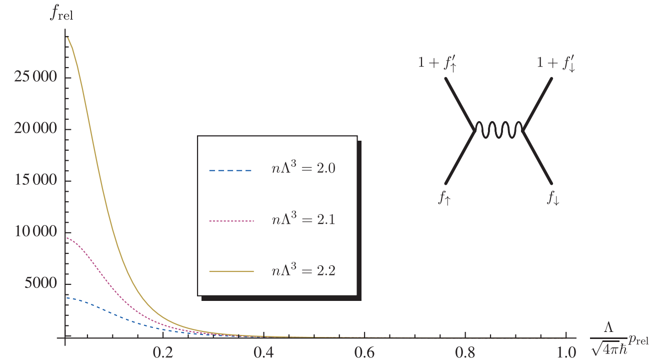

FIG. 4 (color online). A plot of an effective relative momentum occupation, $f_{\text{rel}}(p_{\text{rel}})$, for three values of the parameter $n\Lambda^3$. The figure clearly shows a sharp increase in f_{rel} as one approaches the critical temperature. The Feynman diagram indicates that the interspin scattering rate is increased by the Bose enhancement factors, $(1 + f'_\uparrow)(1 + f'_\downarrow)$, for the outgoing states.

where $f^0_{\mathbf{p}} = (\exp[(\epsilon_{\mathbf{p}} - \mu)/k_B T] - 1)^{-1}$ is the equilibrium Bose distribution, μ is the chemical potential, $f_{\mathbf{p}\sigma}(\mathbf{r}, t) = (\exp[\epsilon_{\mathbf{p}} - \mu_\sigma(\mathbf{r})/k_B T_\sigma(\mathbf{r})] - 1)^{-1}$ is the local equilibrium distribution, $\partial_\epsilon f^0_{\mathbf{p}} = -f^0_{\mathbf{p}}(1 + f^0_{\mathbf{p}})/k_B T$, and $\phi_{\mathbf{p}\sigma}$ describes the response to the spatial inhomogeneities in $f_{\mathbf{p}\sigma}$ and contains all dissipative effects. This parametrization represents an expansion in the ratio of the mean-free path to spatial gradients [15].

Linearizing the Boltzmann equations with respect to $\phi_{\mathbf{p}\sigma}$ and gradients in $f_{\mathbf{p}\sigma}(\mathbf{r})$, we find that, for our choice of scattering lengths, the equation for the spin distribution $n_\uparrow - n_\downarrow$ decouples from the equation for the total distribution $n_\uparrow + n_\downarrow$. We consider the linear response of the spin distribution to spin forces $\mathbf{f}_s$, gradients in the spin chemical potential μ_s, and spin temperature T_s independently from the response to the average forces; i.e., we consider the spin-dependent forces $\mathbf{f}_\sigma = \sigma \mathbf{f}_s/2$ and $\nabla T_\sigma = \sigma \nabla T_s/2$. The linearized drift terms in the left-hand side of Eq. (2) are proportional to ∇T_s and $\nabla \mu_s$, but they are not independent thermodynamic forces because the chemical potential has dependence on the density and temperature, $\mu_\sigma = \mu_\sigma(n_\sigma, T_\sigma)$. We therefore transform the drift terms using the Gibbs-Duhem relation, $d\mu_s = -s dT_s + (1/n) dp_s$, and the thermodynamic identity $w = \mu + Ts$, where s is the equilibrium entropy per particle, w is the enthalpy per particle, $p_s = p_\uparrow - p_\downarrow$ is the spin pressure, and we consider the response to the total thermodynamic force $\mathbf{F}_s = \mathbf{f}_s - \nabla p_s/n$ and ∇T_s. Writing the linear-response solution as

$$\phi_{\mathbf{p}s} \equiv \boldsymbol{\phi}_F(\mathbf{p}) \cdot \mathbf{F}_s + k_B \boldsymbol{\phi}_T(\mathbf{p}) \cdot (-\nabla T_s), \tag{5}$$

the linearized collision integral in the spin equation can be written as $C_{\mathbf{p}s}(\phi_s) \equiv C_{\mathbf{p}}(\boldsymbol{\phi}_F) \cdot \mathbf{F}_s + C_{\mathbf{p}}(\boldsymbol{\phi}_T) \cdot (-\nabla T_s)$. The linearized Boltzmann equation for the spin distribution requires that $\boldsymbol{\phi}_F, \boldsymbol{\phi}_T$ satisfy

$$\partial_\epsilon f^0_{\mathbf{p}} \mathbf{v}_{\mathbf{p}} = C_{\mathbf{p}}(\boldsymbol{\phi}_F), \qquad \partial_\epsilon f^0_{\mathbf{p}} \left(\frac{\epsilon_{\mathbf{p}} - w}{k_B T} \right) \mathbf{v}_{\mathbf{p}} = C_{\mathbf{p}}(\boldsymbol{\phi}_T). \tag{6}$$

Using the solution to Eq. (6), the spin and spin-heat currents are given by

$$\begin{aligned} \mathbf{j}_s &= -\int \frac{d^3 p}{(2\pi\hbar)^3} \partial_\epsilon f^0_{\mathbf{p}} \mathbf{v}_{\mathbf{p}} \phi_{\mathbf{p}s} \\ \mathbf{q}_s &= -\int \frac{d^3 p}{(2\pi\hbar)^3} \partial_\epsilon f^0_{\mathbf{p}} (\epsilon_{\mathbf{p}} - w) \mathbf{v}_{\mathbf{p}} \phi_{\mathbf{p}s}. \end{aligned} \tag{7}$$

To solve Eq. (6), we expand the solutions in a power series, $\boldsymbol{\phi}_F = \sum_{n=0} a_n(\mu, T)(\epsilon_{\mathbf{p}}/k_B T)^n \mathbf{p}$, $\boldsymbol{\phi}_T = \sum_{n=0} b_n(\mu, T) \times (\epsilon_{\mathbf{p}}/k_B T)^n \mathbf{p}$, and take moments of the Boltzmann equation by multiplying Eq. (6) by $(\epsilon_{\mathbf{p}}/k_B T)^n \mathbf{p}$ and integrating over $\mathbf{p}$, resulting in a series of equations of a_n, b_n, which we truncate and solve at the second order. The transport coefficients are readily expressed in terms of the expansion coefficients and the temperature dependence was computed numerically. The Bose enhancement of the spin drag rate in the absence of spin-heat currents, calculated in Refs. [16,17], was computed using the leading-order solution which describes local Bose distributions for the spin-up and -down particles rigidly shifted apart, resulting in a spin current. The second-order solution which we have determined here represents a distortion of the local Bose distribution and is necessary to capture coupled spin and heat flows [18].

We note that σ_s, which determines the spin current driven by external forces, is related to the spin diffusivity D_s, which determines the spin current driven by diffusive forces induced by spin density gradients via $\mathbf{j}_s = -D_s \nabla n_s$, where $n_s = n_\uparrow - n_\downarrow$ is the spin density. This diffusive current tends to return the system to homogeneous equilibrium and must satisfy the Einstein relation, $D_s = \sigma_s/\chi_s$, where $\chi_s = \partial n_s/\partial \mu_s$ is the static spin susceptibility and $\mu_s = \mu_\uparrow - \mu_\downarrow$ is the spin accumulation. We plot the spin diffusivity in Fig. 2 using the noninteracting spin susceptibility. The diffusivity also determines the spin density gradient induced by a spin temperature gradient in the absence of a spin current. For example, for a typical density of $n = 10^{12}$ cm^{-3} at a temperature of $T = 1.5$ μK ($n\Lambda^3 = 2.41$), we find $|\nabla n_s/\nabla T_s| = \chi_s S_s \sim 10^{11}$ μK^{-1} cm^{-3}. For a typical temperature gradient of 10 μK/cm and for a cloud size of 1 mm [6], we find a spin density accumulation of $\delta n_s = 10^{11}$ cm^{-3} , which gives a sizable experimental signal of a $\delta n_s/n = 10\%$.

Similarly, the heat current driven by ∇T_s tends to reduce unequal distributions of energy between spin-up and -down particles. The total dissipation is given by

$$T \partial_t \mathcal{S} = \frac{\sigma_s}{2} \mathbf{F}^2_s + \frac{\kappa'_s}{2T} (\nabla T_s)^2 + \sigma_s S_s \mathbf{F}_s \cdot \nabla T_s, \tag{8}$$

where $\mathcal{S}$ is the total (spin-summed) entropy. It is thus possible to measure κ'_s and S_s by measuring the heating. Furthermore, the last term, analogous to Thompson heating, is sensitive to the relative signs of $\mathbf{F}_s$ and ∇T_s, and allows one to clearly distinguish experimentally the heating contribution coming from the spin-Seebeck coupling. It is important to note that typically experiments are done in the presence of a trapping potential, which introduces spatial dependence in the transport coefficients. The measured values of the transport coefficients should be compared with the trap-averaged values, which differ slightly from the results presented here, but may readily be computed using the Boltzmann formalism. We also note that a spin-dependent temperature gradient can only be established when the intraspin scattering is much stronger than interspin scattering. This can be realized in practice by tuning the spin-dependent scattering lengths using Feshbach resonances.

It is also possible to separate the spin-up and -down atom clouds in an atomic trap by the application of a spin temperature gradient ∇T_s. This results effectively in a spin-dependent force which can be estimated as $F_{\uparrow\downarrow} \approx \pm S_s \nabla T_s$, which must balance the restoring force from the trapping potential, resulting in a separation in the center of mass to the atomic clouds by a distance of $x_s \simeq S_s \nabla T_s / m\omega^2$, where ω is the trapping frequency. For an estimate, we take $m = 1.66 \times 10^{-27}$ kg and $\omega = 2\pi$ Hz and find $x_s \simeq 1$mm, which is within experimental resolution.

For ordinary conductors, one defines a dimensionless figure of merit $ZT = \sigma S^2 T/\kappa$, with σ the conductivity, κ the heat conductivity in the absence of current, and S the thermoelectric Seebeck coefficient, which determines the efficiency of engines based on thermoelectric effects [19]. Analogously, we define $Z_s T = \sigma_s S_s^2 T/\kappa_s$, where $\kappa_s = \kappa_s^l - \sigma_s S_s^2 T$ is the spin-heat conductivity at zero spin current, which is plotted in the inset of Fig. 2 [20]. We plot $Z_s T$ as a function of $n\Lambda^3$ in Fig. 3 and observe an initial decrease as one approaches Bose-Einstein condensation. The quantity $Z_s T$ measures the ratio between the magnitude of the spin-heat coupling and total dissipation; thus, the downturn observed occurs because the spin-heat coupling decreases faster than the total dissipation as one approaches Bose-Einstein condensation.

Our results based on the semiclassical Boltzmann equation are valid outside the critical region of Bose-Einstein condensation. It is known from the theory of dynamical critical phenomena that transport coefficients show anomalous scaling behavior in the critical region [21] which is small but experimentally accessible [22]. To capture the critical fluctuations at the phase transition, one can use the Kubo formula to compute the transport coefficients using the Hamiltonian density $\mathcal{H} = \sum_\sigma \psi_\sigma^\dagger [-\frac{\hbar^2}{2m}\nabla^2 - \mu]\psi_\sigma + \frac{1}{2}\sum_{\sigma\tau} T_{\tau\sigma} \psi_\sigma^\dagger \psi_\tau^\dagger \psi_\tau \psi_\sigma$, where ψ_σ are the bosonic field operators and the strength of the contact interaction is given by the two-body T-matrix element: $T_{\sigma\tau} = 4\pi\hbar^2 a_{\sigma\tau}/m$. The calculation for the spin conductivity, neglecting the vertex corrections in the Kubo formula, was done in Ref. [23], where it was found that the conductivity scales approximately as $\sigma_{sd} \sim \xi \sim (T - T_c)^{-\nu}$, where ξ is the correlation length and $\nu \approx 0.67$ [22]. The same approximation applied to the spin-heat transport coefficients would result in an enhancement in the figure of merit which scale as $Z_s T \sim \xi$. However, whether vertex corrections will significantly change this scaling behavior remains an open question, and warrants further study.

This work was supported by Stichting voor Fundamenteel Onderzoek der Materie (FOM), the Netherlands Organization for Scientific Research (NWO), by the European Research Council (ERC) under the Seventh Framework Program (FP7).

[1] G.E. Bauer, A.H. MacDonald, and S. Maekawa, Solid State Commun. **150**, 459 (2010).
[2] C.M. Jaworski *et al.*, Nature Mater. **9**, 898 (2010); K. Uchida *et al.*, Nature (London) **455**, 778 (2008); K. Uchida *et al.*, Nature Mater. **9**, 894 (2010).
[3] A. Slachter *et al.*, Nature Phys. **6**, 879 (2010).
[4] J. Xiao *et al.*, Phys. Rev. B **81**, 214418 (2010); H. Adachi *et al.*, Appl. Phys. Lett. **97**, 252506 (2010); T.S. Nunner and F. von Oppen, Phys. Rev. B **84**, 020405 (2011).
[5] H. Schmaljohann *et al.*, Appl. Phys. B **79**, 1001 (2004).
[6] R. Meppelink *et al.*, Phys. Rev. Lett. **103**, 095301 (2009).
[7] L. Vichi and S. Stringari, Phys. Rev. A **60**, 4734 (1999).
[8] A. Sommer *et al.*, Nature (London) **472**, 201 (2011),
[9] S.B. Koller *et al.* (to be published).
[10] S.O. Demokritov *et al.*, Nature (London) **443**, 430 (2006); T. Giamarchi *et al.*, Nature Phys. **4**, 198 (2008).
[11] Note that there is no relaxation of the center of mass of the atoms because there is no disorder, and in the absence of a confining potential, the system only reaches a steady state with this choice of forces and temperature gradients.
[12] H. Smith and H.H. Jensen, *Transport Phenomena* (Oxford University Press, New York, 1989).
[13] G.M. Bruun *et al.*, Phys. Rev. Lett. **100**, 240406 (2008).
[14] We note that for this choice of scattering lengths, there is no ferromagnetic phase transition in the normal phase.
[15] L. Pitaevski and E.M. Lifshitz, *Physical Kinetics* (Pergamon, New York, 1981), 1st ed.
[16] R.A. Duine and H.T.C. Stoof, Phys. Rev. Lett. **103**, 170401 (2009).
[17] H.J. van Driel, R.A. Duine, and H.T.C. Stoof, Phys. Rev. Lett. **105**, 155301 (2010).
[18] The correction to the spin drag previously calculated is less than 1% and thus negligible.
[19] G. Mahan, *Solid State Physics* (Academic, New York, 1997), Vol. 51.
[20] Note that the Wiedemann-Franz law that relates the charge conductivity to thermal conductivity for electrons in solid-state systems is not applicable to our cold-atom Bose system.
[21] B.I. Halperin, Phys. Rev. B **11**, 178 (1975); P.C. Hohenberg and B.I. Halperin, Rev. Mod. Phys. **49**, 435 (1977).
[22] T. Donner *et al.*, Science **315**, 1556 (2007).
[23] R. Kittinaradorn *et al.*, arXiv:1107.2024.